



Identification of Seawater Intrusion Using Geoelectrical Method with Wenner-Schlumberger Configuration: A Case Study in Southern Tolonuo Island, North Halmahera Regency, Indonesia

Nikodemus Kalilu

Department of Physics,
Universitas Halmahera
INDONESIA

Bayu Achil Sadjab*

Department of Physics,
Universitas Halmahera
INDONESIA

Masitah Yusniar

Department of Physics,
Universitas Halmahera
INDONESIA

Kurnia

Department of Physics,
Universitas Halmahera
INDONESIA

Elok Surya Pratiwi

Department of Geography,
National Taiwan Normal University
TAIWAN

*Correspondence: E-mail: bayu0604@gmail.com

Article Info

Article history:

Received: March 22, 2022

Revised: June 28, 2022

Accepted: June 30, 2022

Keywords:

Seawater intrusion;
Geoelectric method;
Wenner schlumberger;
RES2DINV software;
Resistivity.

Abstract

Research on seawater intrusion has been carried out on the southern Tolonuo Island, Tobelo Sub-district, North Halmahera Regency, Indonesia using the Wenner-Schlumberger configuration resistivity geoelectric method supported by the Naniura NRD 300 HF tool, this study aims to determine the distribution pattern of seawater intrusion and to determine the resistivity value of each subsurface rock layer in the study area. The measurement results are processed using the RES2DINV software to obtain a 2-D pseudo resistivity section that describes the distribution value of the layer that the soil surface is shown in color images. The measurement results on line 1 show that there is seawater intrusion with a resistivity value range of 0.338 m - 2.44 m which is at 4 – 20 meters with a certain pattern, line 2 also has sea water intrusion at a depth of 5 m – 20 m with a resistivity value of 1.31 Ω m – 6.50 Ω m. On line 3, it is clear that there is a good correlation between the intersection of line 1 and line 2, where there is a low resistivity contrast on the line 1 with a stretch of 35 m – 50 m at a depth of 10 m – 20 m and the line 2 with a span of 80 m - 100 m at a depth of 10 m - 20 m. The distribution pattern of seawater intrusion from the south to the north of Tolonou Village with a wide range of up to 200 meters from residential areas from the shoreline. The research area has layers of clay rock with a resistivity value between 30 – 80 Ω m, and breccia rocks around it with a resistivity value of 100 – 200 Ω m. On the other hand, between clay and breccia there is impermeable rock which is thought to be conglomerate rock with a resistivity value of 200-500 Ω m, besides that in the study area there is also a layer suspected to be a groundwater aquifer layer with a resistivity value (ρ) < 10 m.

Copyright © IJHES 2022, All right reserved

To cite this article: Kalilu, N., Sadjab, B, A., Yusniar, M., Kurnia, and Pratiwi, E, S. (2022). Identification of Seawater Intrusion Using Geoelectrical Method with Wenner-Schlumberger Configuration: A Case Study in Southern Tolonuo island, Tobelo sub-district, North Halmahera Regency, Indonesia. *International Journal of Hydrological and Environmental for Sustainability*, 1(2), 86-96

INTRODUCTION

Seawater intrusion is an event of infiltration or seepage of seawater into groundwater. Seawater intrusion is a problem that often occurs in coastal areas (Kagabu et al., 2013; Lyu et al., 2021; Skelton et al., 2019; Umar Kura et al., 2013). Groundwater is one of the Natural Resources (NR) which has a very important role for human survival because it can meet the supply of clean water suitable for consumption (Kagabu et al., 2013; Nunes et al., 2020; Pender et al., 1998; Skelton et al., 2019; Sobsey

& Pfaender, 2002). The increase in the need for clean water is proportional to the increase in population and the development of an area. As the demand for clean water increases, the exploitation of groundwater will be even greater (Anderson et al., 2009; Zemlicka, 1991).

In coastal areas, the decrease in ground water can cause intrusion or seepage of sea water into the land because groundwater pressure is lower than sea water so that it is the only factor that can interfere with groundwater quality (Bartram & Ballance, 1996; Division of Early Warning and Assessment, 2003; FAO, 2016; Hosono & Masaki, 2020). South Tolonuo Island is one of the islands located in the coastal area with a livelihood as fishermen and farmers. To meet their daily needs, the village community only uses dug well water as the main source for their daily needs including for consumption, while preliminary research shows that the quality of well water has decreased due to the high DHL value, thus indicating the presence of mixing of salts. minerals that are assumed to occur due to seawater intrusion (Jasechko et al., 2020).

To determine the distribution pattern of seawater intrusion and subsurface layers in South Tolonuo Village, Indonesia, this study conducted measurements using the geoelectric method based on differences in resistivity parameters. The resistivity geoelectric method is one method that is quite widely used in the world of exploration, especially groundwater exploration because the resistivity of rock is very sensitive to its water content where the earth is considered a resistor.

METHOD

In this study, a geophysical survey was conducted using a geoelectric with the Wenner-Schulumberger configuration in South Tolonuo Village, Tobelo District, North Halmahera Regency, Indonesia. The survey was conducted directly or at the research location for 1 month, in June 2019. The study was conducted in June because the intensity of rain is small (dry season), so that noise disturbance due to rainwater in the research area will be very small.

Resistivity Method

The geoelectric method can be used properly if there is a resistivity contrast between the mediums. Contrast can be a medium that is relatively conducive to a non-conductive medium, or there are lithological differences. Each type of subsurface rock has a different resistivity value. Each resistivity depends on the density, water content, minerals, salt content, and porosity of the rock (Sadjab et al., 2020). The working principle of geoelectricity is to measure resistivity by flowing an electric current into rock or soil through two current electrodes, then the current is received by two potential electrodes (Prastowo et al., 2019; Siregar & Kurniawan, 2018). The distance between the electrodes can vary according to the specifics of the area and topography, so the resistivity value can be calculated using Ohm's law. Let R be resistance (Ohm); A is the cross-sectional area of the medium (m^2), and L is the length of the medium (m), then based on **Figure 1**, the resistivity of the medium, (Ωm) can be determined using equation 1 (Kumar et al., 2015),

$$\rho = R \frac{A}{L} \quad (1)$$

According to Ohm's law that the resistance R of the medium can be mathematically calculated using equation 2, as

$$R = \frac{\Delta V}{I} \quad (2)$$

Following the potential difference between the edges of the medium ΔV and the injected current I, then the resistivity can be calculated using the equation 3,

$$\rho = \frac{\Delta V}{I} \cdot \frac{A}{L} \quad (3)$$

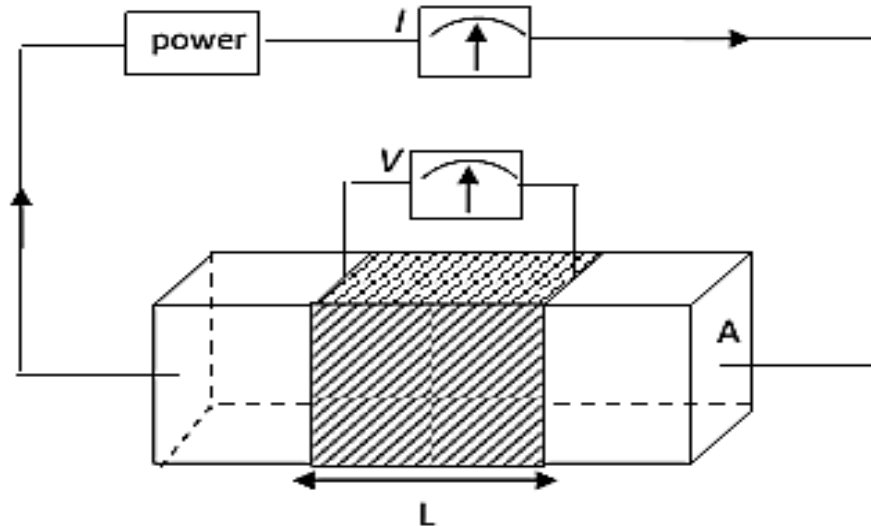


Figure 1. Illustration of medium through which current I , length L and cross-sectional area A

Equation 3 applies to homogeneous media, so the result obtained is the true resistivity. But in practice, the object being measured is the earth or the ground is not homogeneous because of the different types of resistors, so the measured resistivity is the apparent resistivity. The apparent resistivity value depends on the resistivity of the formation layer and the electrode configuration used (Sadjab et al., 2012). The apparent resistivity is a formulated by the following equation 4.

$$\rho_a = K \frac{\Delta V}{I} \tag{4}$$

where K is the geometric factor.

Wenner-Schlumberger Configuration

The Wenner-Schlumberger configuration is a configuration with a system of constant spacing rules with a note that the "n" factor for this configuration is the ratio of the distance between the C1-P1 (or C2-P2) electrodes to the space between P1-P2 as shown in Figure 2 (Raharjo & Sehad, 2018). If the distance between the potential electrodes (P1 and P2) is a , then the distance between the current electrodes (C1 and C2) is $2na + a$. The process of determining the resistivity uses 4 electrodes placed in a straight line, shown in Figure 2 (Kanata & Zubaidah, 2008).

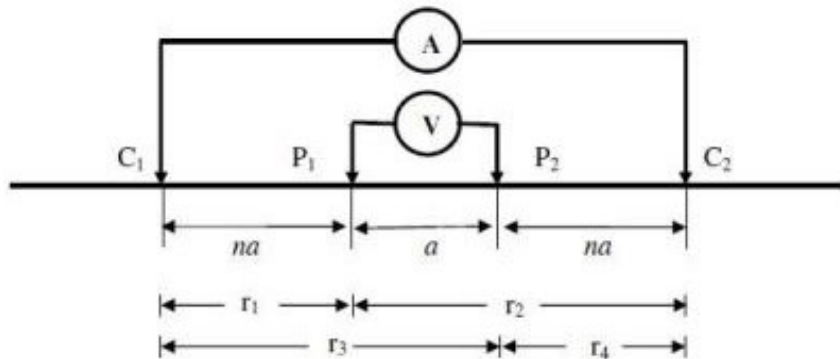


Figure 2. Wenner-Schlumberger configuration electrode position adjustment

The variable n is a multiple to indicate the observed layers. The Wenner-Schlumberger geometric factor can be calculated using equation 5,

$$K = \pi(n+1)a \tag{5}$$

where a is the distance between the electrodes P1 and P2, n is the ratio of the distances between the electrodes C1-P1 and P1-P2 (eg 4a, then $n = 4$) so that all resistivity values obtained from the measurement results are the same as equation 6,

$$\rho_a = \pi(n+1)a \frac{\Delta V}{I} \quad (6)$$

The resistivity values for rock and mineral layers can be seen in **Table 1**.

Table 1. Rock and Mineral Layer Resistivity Value

No	Material Type	Resistivity (Ωm)
1	Clay	1-100
2	Silt	10-200
3	Mudstone	3-70
4	Quartz	$10\text{-}2 \times 10^8$
5	Sandstone	50-500
6	Limestone	100-500
7	lava	$100\text{-}5 \times 10^4$
8	Meteoric Water	30-100
9	Surface water	10-100
10	Groundwater	0,5-300
11	Sea water	0,2
12	Breccia	75-200
13	Andesite Stone	100-200
14	Volcanic Tufa	20-100
15	Conglomerate Rock	$2 \times 10^3\text{-}1 \times 10^4$
16	Basalt Stone	$1 \times 10^3\text{-}1 \times 10^6$
17	Granite Stone	$5 \times 10^3\text{-}1 \times 10^6$
18	Slate	$6 \times 10^2\text{-}4 \times 10^7$
19	Soil	0,60
20	Soil	16,7
21	Sand	0,95
22	Sand	8,3
23	Gravel	100-600

(Source : Data from [W.M. Telford, 1991](#))

Data Collection Techniques

The research was conducted by direct observation and measurements in the field. The research location is approximately 100 meters from the residential area of South Tolonuo Village, Tobelo District, North Halmahera Regency. The study was conducted at 3 measurement points with a line length of 100 meters and 150 meters. The measurement at point 1, the length of the line is 150 meters, the direction of the stretch is north to south, residential areas. The point 2 community plantation area. And point 3 stretching from east to west, namely from the plantation area to the residential area can be seen in **Figure 3**, the distance from point 1 to point 2 is 100 meters and line 3 is crosswise or the intersection between line 1 and line 2. Conditions of the research area for points 1, 2, and 3 are relatively flat covering the residents' plantations to residential areas, with sunny weather at the time of measurement.



Figure 3. Research site map and research survey design

The research process starts from preparation, literature study, data acquisition, processing using software and analysis and interpretation. Graphically, the research procedure can be shown in **Figure 4**. Preparation begins with a literature study of the geological data of the research area and information related to brackish well water in South Tolonuo Village, by conducting interviews with villagers, as well as conducting field surveys (Nafian et al., 2022). Furthermore, data acquisition is carried out, with data acquisition covering the implementation of data collection activities in the field, in this case using a geoelectric tool to obtain the value of the current injection (I) and the value of the voltage (V), the current and voltage injection value data are then processed to obtain the resistivity value which is then processed. reprocessed using RES2DINV software to get a 2D cross-sectional model (Jamaluddin & Umar, 2018). This software works based on the inversion technique related to the last square method (Pratiwi et al., 2019). RES2DINV is an exact algorithm which is considered good for inversion of 2D resistivity data, and there is good scientific literature where the RMS of 2D electrical imaging is greater than 10% (Satriani et al., 2012). The results of the processing in the form of a 2D cross-section of rock layer resistivity in the form of color images were then analyzed and interpreted to determine the distribution pattern of seawater intrusion and the type of subsurface layering in Tolonuo Selatan Village, Tobelo District, North Halmahera Regency, Indonesia.

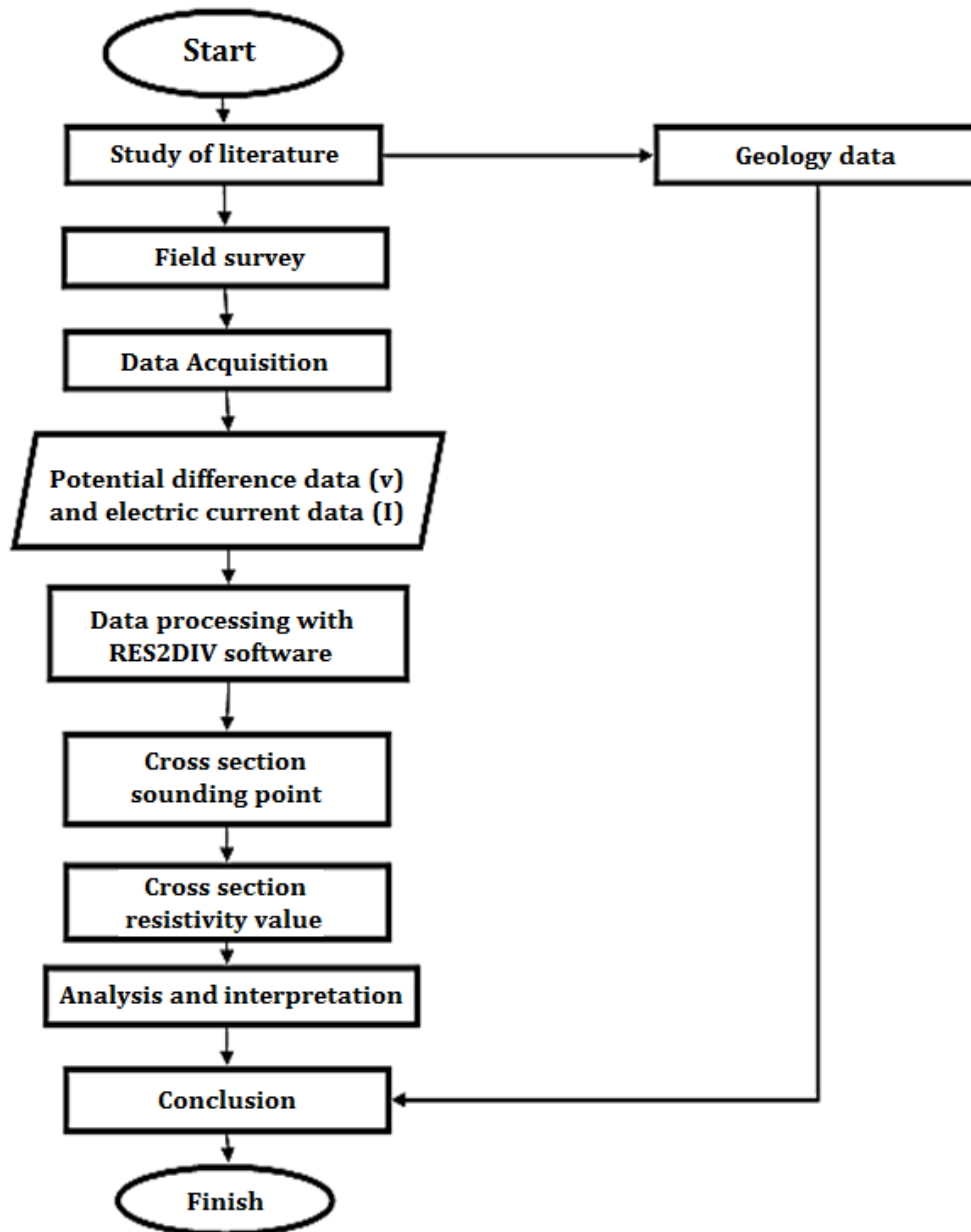


Figure 4. Research Flowchart

RESULTS AND DISCUSSION

The physiography of the research area is divided into 3 parts, namely the Mandala of West Halmahera, the Mandala of East Halmahera and the Quaternary Volcano (Hall, 2018). The dominant rocks in the study area include Alluvium, Tufa, Andesite, Sediment, Clay, Marble, Conglomerate, Ultramafic, Breccia, and Metamorphic Rocks (Figure 5).

The stratigraphy of the study area consists of 17 formations that range from pre-Cretaceous to Holocene ages. The rock structure consists of Sedimentary Rocks with Dodaga Formation (Kd), Limestone Unit, Dogosagu Formation (Tped), Conglomerate Unit (Tpec), Tutuli Formation (Tomt), Conglomerate (Tmpc), Tingteng Formation (Tmpt), Veda Formation (Tmpw), and Coral Limestone (Ql). Surface Deposits with Alluvium and Coastal Deposits (Qa). Volcanic Rocks with the composition of Bacan Formation (Tomb), Kayasa Formation (Qpk), Tufa Unit (Qht), Volcanic Holocene Rock (Qhv). Igneous rocks consist of Ultrabasic Rock (Ub), Gabbro (Gb) and Diorite (Di) (Figure 5).

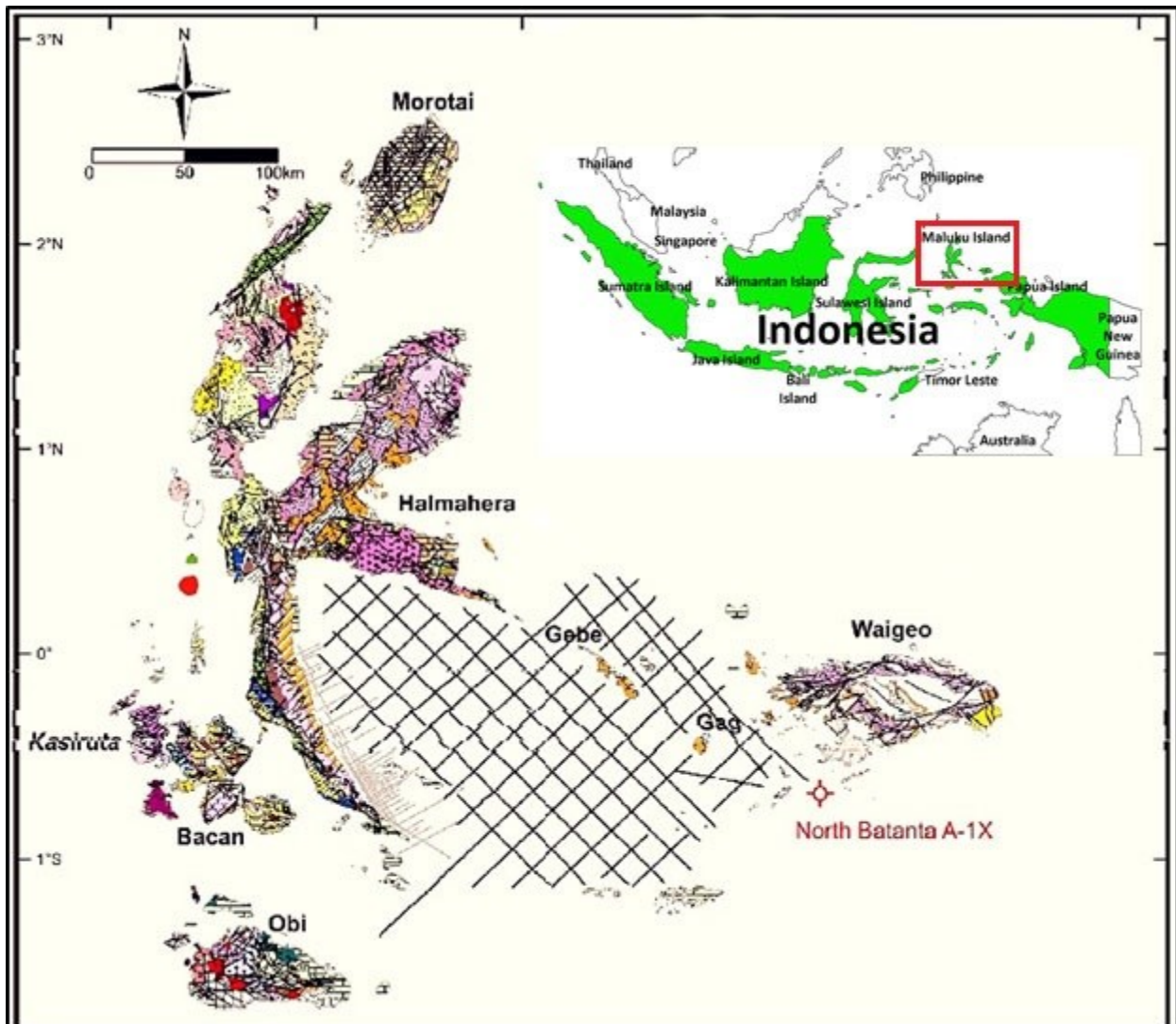


Figure 5. Geological Map of Halmahera Island and Surrounding Areas (Hall, 2018)

2D Cross-sectional Resistivity of Rock and Mineral Layers

The data obtained from direct observation in the field are current (I), voltage (ΔV), apparent resistivity (ρ), datum point data, spacing, and number of layers. The data obtained was then processed using the RES2DINV software for the three lines around the residential area of South Tolonuo Village. The result of this software processing is in the form of a 2-D inversion which can then be saved in (xyz) format. Data in (xyz) format consists of accumulated electrode distance, actual resistivity value, current penetration depth, and subsurface conductivity based on the measurement results.

Line 1 is located at the coordinates $1^{\circ}46'47''$ LU and $128^{\circ} 0'2''$, This line point is 100 meters from the beach. Based on the resistivity contour image processing with the RES2DINV software (Figure 6), it can be seen that there is a resistivity contrast with the green color image which has a resistivity value between $5,5 \Omega\text{m} - 7 \Omega\text{m}$ which is at a depth of 9 – 20 meters, this layer is interpreted as a groundwater aquifer layer. , this is also evidenced by the water source excavated close to the line point has a depth of 10 - 20 meters. At a depth of 2-10 meters below the surface there are clay rocks around the groundwater aquifer (yellow color image) with a resistivity value between $30 - 80 \Omega\text{m}$, then it is seen that there are water-resistant rocks with resistivity values between $100 - 300 \Omega\text{m}$ these rocks are thought to be conglomerate rocks forming bolder-bolders which are geologically present at the research site, because of the presence of these impermeable rocks, causing Groundwater collects and enters the groundwater aquifer. Line 1 also shows the presence of seawater intrusion, this can be seen from the resistivity contrast with the dark blue color image to

light blue with a resistivity value range of $0.338 \Omega\text{m}$ - $2.44 \Omega\text{m}$, the color image of this layer starts from a depth of 4 – 20 meters with a certain pattern, this layer is interpreted as a layer of salt water that has entered the subsurface groundwater aquifer through the intrusion process. This interpretation is strengthened because of the shape of the flow pattern of seawater intrusion that forms spots, and is also supported by testing the groundwater of the line that has been contaminated by saltwater due to the seawater intrusion process.

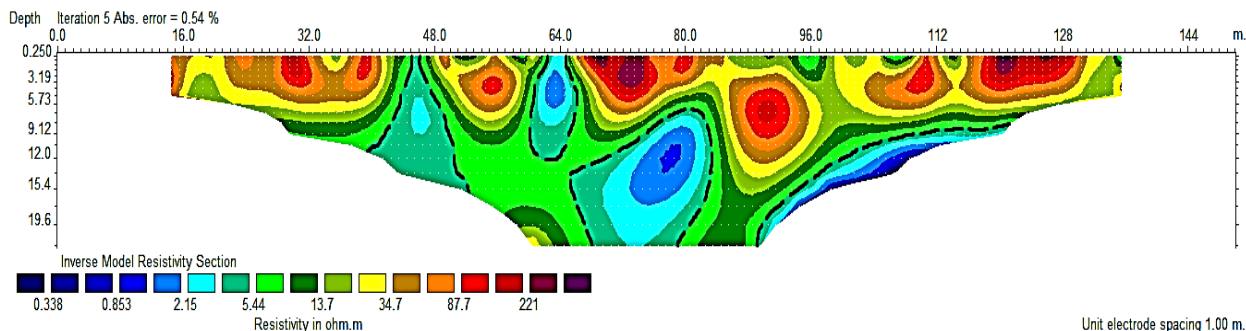


Figure 6. 2D Section Resistivity of Rock Layer on Line 1

Line 2 is located at coordinates $1^{\circ}46'14.42''\text{LU}$ and $128^{\circ}50.49''\text{BT}$. This trajectory point is parallel to line 1 with a distance between trajectories of 100 m, based on the geology of the research area in **Figure 7** the yellow to red color image as in the first trajectory is interpreted as clay rock that passes water which is at a depth of 2 – 10 m from the surface with a resistivity value $36 \Omega\text{m}$ – $80 \Omega\text{m}$, then at a depth of 3-12 meters there are breccia rocks with resistivity values between $100 - 200 \Omega\text{m}$ (brown color image), between clay rocks and breccias there are also conglomerate rocks, this is correlated with the stratigraphic arrangement of the study area, these rocks are shown in red images to purple with a resistivity value between $200 - 500 \Omega\text{m}$, form bolder-bolder and is this rock that is impermeable to water. While the light blue to dark blue color images are very large seawater intrusions when viewed from line 1, the intrusion (**Figure 6**) is still small at a stretch of 80 m – 120 m and a depth of 10 m – 20 m, while on line 2 there are already seawater intrusion on a stretch of 35 m – 112 m with a depth of 5 m – 20 m with a resistivity value $1.31 \Omega\text{m}$ – $6.50 \Omega\text{m}$ this layer is interpreted as salt water that has entered the subsurface groundwater aquifer.

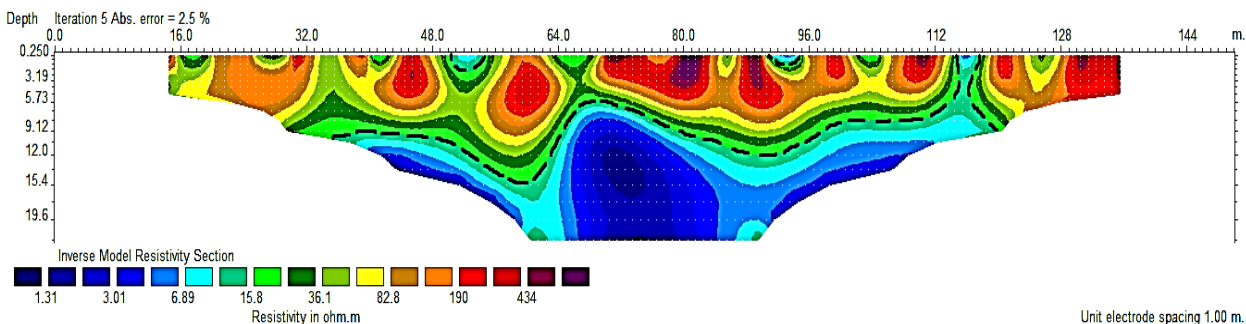


Figure 7. 2D Section Resistivity of Rock Layer on Line 2

Line 3 is located at coordinates $1^{\circ}46'39''\text{LU}$ and $128^{\circ}0'39''$. This line is the result of measurements that are perpendicular to cross line 1 and 2, this trajectory is carried out in order to obtain a direct correlation or relationship between trajectory 1 and trajectory 2. Based on the pseudo 2-D cross-section of the resistivity contour processed with the RES2DINV software (**Figure 8**), it is clear that there is a good correlation between the intersection of line 1 and line 2, where there is a low resistivity contrast on the right side (line 1) with a stretch distance of 35 m – 50 m at a depth of 10m – 20m and the left side (line 2) with a stretch distance of 80 m-100 m at a depth of 10m – 20m, this shows that there have been indications of seawater intrusion on the two lines, this interpretation is shown by the contrast blue resistivity image with low resistivity value ($\rho < 5 \Omega\text{m}$) with a

distribution pattern of sea water intrusion from the south to the north of Tolonou Village with a wide range of up to 200 meters from residential areas from the beach. Based on the pseudo 2-D cross-section of line 3, it can also be seen that there is a suitability of impermeable rock boundaries with high resistivity values as shown in the pseudo 2-D cross-section of lines 1 and 2 (**Figure 8**).

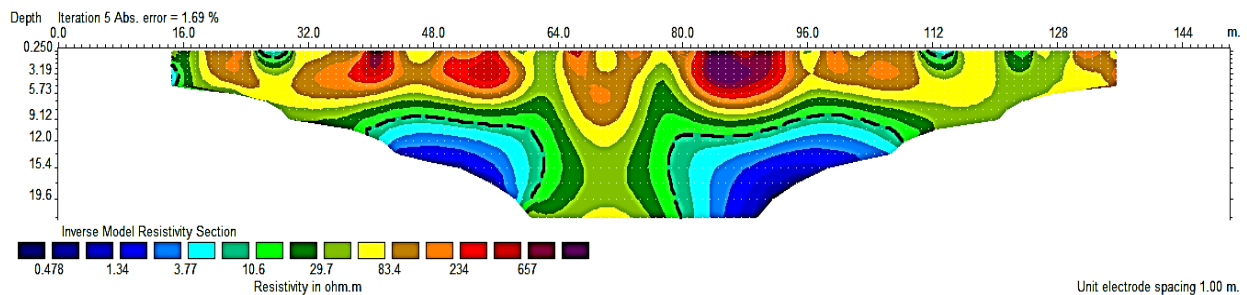


Figure 8. 2D Section Resistivity of Rock Layer on Line 3

CONCLUSION

Based on the results of data analysis, it was concluded that at a distance of 100 m to 200 m from the shoreline it was contaminated with seawater intrusion on line 1, seawater intrusion occurred at a depth of 4-20 meters with a resistivity value $0.338 \Omega\text{m} - 2.44 \Omega\text{m}$, while on line 2 occurs at a stretch of 35 m – 112 m with a depth of 5 m – 20 m with a resistivity value $1.31 \Omega\text{m} - 6.50 \Omega\text{m}$, and line 3 shows a good correlation between line 1 and 2, this is because this line intersects the two lines. The distance of community houses from the shoreline is only about 5 m, the nearest and the furthest is about 30 m. Therefore, it is indicated that the source of clean water on South Tolonuo Island, Tobelo District, North Halmahera Regency has experienced intrusion with a distribution pattern from the south to the north of the village, with a wide range of up to 200 meters from residential areas from the coast. In addition, based on the results of the 2-D pseudo resistivity section below the surface for each line, in the study area there is a layer of clay rock with a resistivity value between $30 - 80 \Omega\text{m}$. Then there are also breccia rocks around it with resistivity values between $100 - 200 \Omega\text{m}$, between clay and breccia there is impermeable rock which is thought to be conglomerate rock with resistivity value $200 - 500 \Omega\text{m}$, this rock layer has a correlation with the stratigraphic arrangement of the research area, besides that in the research area there is also a layer that is suspected to be a groundwater aquifer layer with a resistivity value $(\rho) < 10 \Omega\text{m}$.

ACKNOWLEDGMENT

The authors are grateful to Department of Physics, Halmahera University for providing the opportunities and support to conduct research.

CONFLICTS OF INTEREST

The authors declare no conflict of interest concerning the publication of this article. The authors also confirm that the data and the article are free of plagiarism.

REFERENCES

- Anderson, R., Bartram, J., Chartier, Y., Gordon, B., Hope, L., Menucci, E. J. D. L., Plotkin, B., & Sheffer, M. (2009). Hygiene and Sanitation in Aviation. In *World Health Organization* (Vol. 17, Issue 3).
- Bartram, J., & Ballance, R. (1996). Water Quality Monitoring - A Practical Guide to the Design and Implementation of Freshwater Quality Studies and Monitoring Programmes. In *United Nations Environment Programme and the World Health Organization (UNEP/WHO)* (Vol. 16, Issue 48).

- Division of Early Warning and Assessment. (2003). *Groundwater and its Susceptibility to Degradation*. UNEP.
- FAO. (2016). Thematic Papers on Groundwater. In *Groundwater Governance – A Global Framework for Action*.
- Hall, R. (2018). *Neogene history of collision in the Halmahera region, Indonesia*. <https://doi.org/10.29118/ipa.2461.g.014>
- Hosono, T., & Masaki, Y. (2020). Post-seismic hydrochemical changes in regional groundwater flow systems in response to the 2016 Mw 7.0 Kumamoto earthquake. *Journal of Hydrology*, 580(November 2019), 124340. <https://doi.org/10.1016/j.jhydrol.2019.124340>
- Jamaluddin, & Umar, E. P. (2018). Identification of subsurface layer with Wenner-Schlumberger arrays configuration geoelectrical method. *IOP Conference Series: Earth and Environmental Science*, 118(1). <https://doi.org/10.1088/1755-1315/118/1/012006>
- Jasechko, S., Perrone, D., Seybold, H., Fan, Y., & Kirchner, J. W. (2020). Groundwater level observations in 250,000 coastal US wells reveal scope of potential seawater intrusion. *Nature Communications*, 11(1), 1–9. <https://doi.org/10.1038/s41467-020-17038-2>
- Kagabu, M., Shimada, J., Delinom, R., Nakamura, T., & Taniguchi, M. (2013). Groundwater age rejuvenation caused by excessive urban pumping in Jakarta area, Indonesia. *Hydrological Processes*, 27(18), 2591–2604. <https://doi.org/10.1002/hyp.9380>
- Kanata, B., & Zubaidah, T. (2008). Aplikasi Metode Geolistrik Tahanan Jenis Konfigurasi Wenner. *Teknik Elektro Fakultas Teknik Universitas Mataram*, 7(2), 84–91.
- Kumar, N., Rao, R., & Naganjaneyulu, K. (2015). Electrical resistivity imaging (ERI) using multielectrodes for studying sub- surface formations in Cauvery plains. *Advances in Applied Science Research*, 6(5), 47–53.
- Lyu, H. M., Shen, S. L., Wu, Y. X., & Zhou, A. N. (2021). Calculation of groundwater head distribution with a close barrier during excavation dewatering in confined aquifer. *Geoscience Frontiers*, 12(2), 791–803. <https://doi.org/10.1016/j.gsf.2020.08.002>
- Nafian, M., Gunawan, B., Permana, N. R., & Umam, R. (2022). Identification of the Subsurface Structure of Geothermal Working Area of the Hamiding Mountain , North Maluku through Land Surface Temperature (LST) Data and Forward Modeling with the Gravity Method. *J. Nat. Scien. & Math. Res*, 8(1), 10–19.
- Nunes, L. J. R., Loureiro, L. M. E. F., Sá, L. C. R., & Silva, H. F. C. (2020). Sugarcane industry waste recovery: A case study using thermochemical conversion technologies to increase sustainability. *Applied Sciences (Switzerland)*, 10(18). <https://doi.org/10.3390/APP10186481>
- Pender, S. M., Boland, G. W., & Lee, M. J. (1998). The incidental nonhyperfunctioning adrenal mass: An imaging algorithm for characterization. *Clinical Radiology*, 53(11), 796–804. [https://doi.org/10.1016/S0009-9260\(98\)80189-X](https://doi.org/10.1016/S0009-9260(98)80189-X)
- Prastowo, R., Huda, S., Umam, R., Jermsittiparsert, K., Prasetyo, A. E., Tortop, H. S., & Syazali, M. (2019). Academic Achievement And Conceptual Understanding Of Electrodynamics: Applications Geoelectric Using Cooperative Learning Model. *Jurnal Ilmiah Pendidikan Fisika Al-Biruni*, 8(2), 165–175. <https://doi.org/10.24042/jipfalbiruni.v0i0.4614>
- Pratiwi, E. S., Sartohadi, J., & Wahyudi. (2019). Geoelectrical Prediction for Sliding Plane Layers of Rotational Landslide at the Volcanic Transitional Landscapes in Indonesia. *IOP Conference Series: Earth and Environmental Science*, 286(1). <https://doi.org/10.1088/1755-1315/286/1/012028>
- Raharjo, S. A., & Sehad, M. (2018). Eksplorasi Potensi Pasir Besi di Pesisir Barat Kecamatan Nusawungu Kabupaten Cilacap Berdasarkan Data Resistivitas Batuan Bawah Permukaan. *Jurnal Fisika Dan Aplikasinya*, 14(3), 51. <https://doi.org/10.12962/j24604682.v14i3.3613>

- Sadjab, Bayu A., . A., & Tanauma, A. (2012). Pemetaan Akuifer Air Tanah Di Sekitar Candi Prambanan Kabupaten Sleman Daerah Istimewa Yogyakarta Dengan Menggunakan Metode Geolistrik Tahanan Jenis. *Jurnal MIPA*, 1(1), 37. <https://doi.org/10.35799/jm.1.1.2012.432>
- Sadjab, Bayu Achil, Indrayana, I. P. T., Iwamony, S., & Umam, R. (2020). Investigation of The Distribution and Fe Content of Iron Sand at Wari Ino Beach Tobelo Using Resistivity Method with Werner-Schlumberger Configuration. *Jurnal Ilmiah Pendidikan Fisika Al-Biruni*, 9(1), 141–160. <https://doi.org/10.24042/jipfalbiruni.v9i1.5394>
- Satriani, A., Loperte, A., Imbrenda, V., & Lapenna, V. (2012). Geoelectrical surveys for characterization of the coastal saltwater intrusion in metapontum forest reserve (Southern Italy). *International Journal of Geophysics*, 2012. <https://doi.org/10.1155/2012/238478>
- Siregar, R. N., & Kurniawan, W. B. (2018). 2D Interpretation of Subsurface Hot Spring Geothermal Structure in Nyelanding Village Through Schlumberger Geoelectricity Configuration Method. *Jurnal Ilmiah Pendidikan Fisika Al-Biruni*, 7(1), 81. <https://doi.org/10.24042/jipfalbiruni.v7i1.2324>
- Skelton, A., Liljedahl-Claesson, L., Wästeby, N., Andrén, M., Stockmann, G., Sturkell, E., Mörth, C. M., Stefansson, A., Tollefsen, E., Siegmund, H., Keller, N., Kjartansdóttir, R., Hjartarson, H., & Kockum, I. (2019). Hydrochemical Changes Before and After Earthquakes Based on Long-Term Measurements of Multiple Parameters at Two Sites in Northern Iceland—A Review. *Journal of Geophysical Research: Solid Earth*, 124(3), 2702–2720. <https://doi.org/10.1029/2018JB016757>
- Sobsey, M. D., & Pfaender, F. K. (2002). Evaluation of the H₂S Method for Detection of Fecal Contamination of Drinking Water. In *Public Health* (p. 44). http://www.who.int/water_sanitation_health/dwq/WSH02.08.pdf
- Umar Kura, N., Firuz Ramli, M., Azmin Sulaiman, W. N., Ibrahim, S., Zaharin Aris, A., & Mustapha, A. (2013). Evaluation of factors influencing the groundwater chemistry in a small tropical Island of Malaysia. *International Journal of Environmental Research and Public Health*, 10(5), 1861–1881. <https://doi.org/10.3390/ijerph10051861>
- W.M. Telford, L. P. G. and R. E. S. (1991). Applied geophysics (second edition). In *Cambridge University Press*.
- Zemlicka, J. (1991). Fluoride in drinking water [5]. In *Chemical and Engineering News* (Vol. 69, Issue 4).